

Molecular dynamics with multiple time scales: The selection of efficient reference system propagators

Steven J. Stuart, Ruhong Zhou, and B. J. Berne

Department of Chemistry and the Center for Biomolecular Simulation, Columbia University, New York, New York 10027

(Received 15 March 1996; accepted 18 April 1996)

Several heuristic rules are developed to assist in the implementation of the reversible reference system propagator algorithm (rRESPA). This is done through the use of examples, illustrating the use of properly chosen rRESPA splits of various types, as well as the dangers associated with improperly chosen ones. It is concluded that a particle-based rRESPA split should be used only when there is a great disparity in particle masses, and that a force-based split should be used only when there is no persisting opposition between forces in the system which are integrated with different time steps. © 1996 American Institute of Physics. [S0021-9606(96)00928-2]

I. INTRODUCTION

As with many other areas of computational chemistry, molecular dynamics (MD) simulations have progressed at a remarkable pace over the past few decades. Systems which are suitable for MD simulation are constantly growing in both size and complexity, while the simulation times are also increasing relentlessly. One of the most important factors responsible for this continued progress, of course, is the astounding rate of improvement in computer power. These “brute force” gains have been further compounded, though, by the development of faster algorithms and integrators. Recent techniques such as the fast multipole method¹ and the reversible reference system propagator algorithm (rRESPA)² accelerate simulations by up to a factor of 15 (Ref. 3)—roughly equivalent to waiting seven years for faster computer hardware.⁴

Multiple-time-scale methods such as rRESPA allow the more slowly varying components of a system to be integrated with a fairly long time step, while still using smaller time steps for the components which are moving most rapidly. This results in faster simulation speeds than are obtainable using single-time-step methods, and the time savings can be used to study larger systems, for longer simulation times. Various implementations of the rRESPA method have been applied to a wide variety of systems,^{2,3,5–17} resulting in speedups by factors of 4 to 15.

Although rRESPA is quite simple to implement, it requires a decision about which parts of the system are to be integrated with which time steps. In some cases, a clear disparity between strong and weak forces or heavy and light particles makes the choice obvious. For others, choosing the best partitioning of the system is more of an art than an exact science. Still, this decision can have extremely important consequences, and an improper choice can result in a less than optimally efficient propagator, or even one which is worse than the original single-time-step method.

This paper is an attempt to provide some guidelines for use when applying rRESPA to new systems. By considering several example systems, and comparing rRESPA propagators which do not work to those which do, we develop some

general principles which should help in avoiding inefficient rRESPA propagators.

In Sec. II we first review the theory behind the rRESPA propagator, and derive two commonly used examples. One of these partitions the system forces, while the other performs a partition based on particle identities. In Sec. III we apply variations on these propagators to four different model systems, pointing out what makes for a successful implementation of the rRESPA method. Section IV summarizes the lessons learned from these different examples, and presents some general conclusions for use in developing new rRESPA propagators.

II. THEORY

A molecular dynamics trajectory involves propagating the state of a system forward in time, where the state $\Gamma(t)$ specifies the individual particles' positions and momenta at time t ,

$$\Gamma(t) = (\{x_i(t)\}, \{p_i(t)\}). \quad (1)$$

The time propagation is handled by an operator $G(t)$, with the property that

$$\Gamma(\Delta t) = G(\Delta t)\Gamma(0). \quad (2)$$

This operator $G(t)$ is generally some approximation to the true classical propagator $U(t)$,

$$U(t) = e^{i\mathcal{L}t}, \quad (3)$$

where

$$i\mathcal{L} = \{ , H \} = \sum_{i=1}^N \left[v_i \frac{\partial}{\partial x_i} + \frac{F_i}{m_i} \frac{\partial}{\partial v_i} \right] \quad (4)$$

is the Liouvillian for a system with N degrees of freedom, expressed in Cartesian coordinates. The first term inside the sum above is responsible for advancing the positions x_i in time by an amount proportional to the velocities v_i ; the second term advances the velocities in proportion to the accelerations F_i/m_i .

The reversible reference system propagator algorithm is a prescription for generating a discretized propagator $G(\Delta t)$

which reversibly integrates different components of the system under two (or more) different time steps. To accomplish this, the Liouvillian is first divided into a “slow” and a “fast” piece.

$$i\mathcal{L} = i\mathcal{L}_s + i\mathcal{L}_f. \quad (5)$$

Then by performing a symmetrical Trotter factorization¹⁸ of the classical propagator, we arrive at an approximation to $U(\Delta t)$,

$$G(\Delta t) = e^{i\mathcal{L}_s\Delta t/2} e^{i\mathcal{L}_f\Delta t} e^{i\mathcal{L}_s\Delta t/2}, \quad (6)$$

which is accurate to $\mathcal{O}(\Delta t^3)$. The approximation results from the fact that $\exp(i\mathcal{L}_s t)$ and $\exp(i\mathcal{L}_f t)$ do not necessarily commute.

If we now factor the inner term in this propagator into n identical pieces, we obtain

$$G(\Delta t) = e^{i\mathcal{L}_s\Delta t/2} [e^{i\mathcal{L}_f\delta t}]^n e^{i\mathcal{L}_s\Delta t/2}, \quad (7)$$

where $\delta t = n\Delta t$. This smaller time step δt is used to integrate the parts of the dynamics advanced by $i\mathcal{L}_f$, while the larger time step Δt is used to advance the terms affected by $i\mathcal{L}_s$. This symmetrical Trotter factorization can be repeated as many times as desired, and at least one more factorization of the inner propagator is typically required to separate the position and velocity components of the propagator. This final subdivision generates a velocity Verlet-like integrator,² and will be illustrated in the following section. As long as the symmetry of the propagator is preserved, the operator $G(\Delta t)$ will generate explicitly time-reversible dynamics.²

Clearly the choice of how to divide the Liouvillian in Eq. (5) is critical, and the most useful split is often dictated by the physics of the problem at hand. Occasionally, however, several different choices seem appropriate, and sometimes the most obvious factorization does not turn out to be the most efficient. The aim of this paper is to provide some guidelines for choosing a rRESPA split which is likely to produce accurate and efficient simulations. This will be done primarily through the discussion of examples in Sec. III. First, however, we describe two different categories of rRESPA propagators which will prove useful in the discussion which follows.

A. Force-based RESPA split

For a system which interacts with itself via pairwise forces, the full Liouvillian of Eq. (4) can be written

$$i\mathcal{L} = \sum_i \left[v_i \frac{\partial}{\partial x_i} + \frac{1}{2} \sum_{j \neq i} \frac{F_{ij}}{m_i} \frac{\partial}{\partial v_i} \right], \quad (8)$$

where $F_{ij} = -F_{ji}$ represents the pair force acting between atoms i and j . If these forces are separable into two groups which act on different time scales, we may divide the Liouvillian correspondingly. The “slow” component of the Liouvillian includes the effect of the slow forces on the particle velocities,

$$i\mathcal{L}_s = \frac{1}{2} \sum_i \sum_{j \neq i} \frac{F_{ij}^{(s)}}{m_i} \frac{\partial}{\partial v_i} \equiv \frac{F^{(s)}}{m} \frac{\partial}{\partial v}, \quad (9)$$

and the “fast” component includes the effect of the fast forces on the velocities, as well as the effect of the velocities on the positions,

$$\begin{aligned} i\mathcal{L}_f &= \sum_i \left[v_i \frac{\partial}{\partial x_i} + \frac{1}{2} \sum_{j \neq i} \frac{F_{ij}^{(f)}}{m_i} \frac{\partial}{\partial v_i} \right] \\ &\equiv v \frac{\partial}{\partial x} + \frac{F^{(f)}}{m} \frac{\partial}{\partial v}, \end{aligned} \quad (10)$$

where we require that

$$F_{ij}^{(s)} + F_{ij}^{(f)} = F_{ij}. \quad (11)$$

Using this decomposition of the Liouvillian in Eq. (7), we obtain a propagator of the form

$$\begin{aligned} G(\Delta t) &= \exp\left(\frac{\Delta t}{2} \frac{F^{(s)}}{m} \frac{\partial}{\partial v}\right) \left[\exp\left(\delta t v \frac{\partial}{\partial x} + \delta t \frac{F^{(f)}}{m} \frac{\partial}{\partial v}\right) \right]^n \exp\left(\frac{\Delta t}{2} \frac{F^{(s)}}{m} \frac{\partial}{\partial v}\right). \end{aligned} \quad (12)$$

To use this propagator in an MD simulation, the inner propagator must be split once more, in order to decouple the position and velocity operators. This is done with another Trotter factorization, giving a velocity Verlet-like inner propagator,

$$\begin{aligned} G(\Delta t) &= \exp\left(\frac{\Delta t}{2} \frac{F^{(s)}}{m} \frac{\partial}{\partial v}\right) \left[\exp\left(\frac{\delta t}{2} \frac{F^{(f)}}{m} \frac{\partial}{\partial v}\right) \right. \\ &\quad \times \exp\left(\delta t v \frac{\partial}{\partial x}\right) \exp\left(\frac{\delta t}{2} \frac{F^{(f)}}{m} \frac{\partial}{\partial v}\right) \left. \right]^n \\ &\quad \times \exp\left(\frac{\Delta t}{2} \frac{F^{(s)}}{m} \frac{\partial}{\partial v}\right). \end{aligned} \quad (13)$$

[Note that this step introduces additional errors of order $\mathcal{O}(n\delta t^3) = \mathcal{O}(\Delta t\delta t^2)$, which are smaller than the $\mathcal{O}(\Delta t^3)$ errors introduced at this point in a derivation of the pure velocity Verlet propagator.] With the propagator in this form, a trajectory can be generated from an initial state $\Gamma(0)$ through repeated application of the operator identity

$$e^{c(\partial/\partial q)} f(q) = f(q+c). \quad (14)$$

Thus the propagator in Eq. (13) produces the following dynamics algorithm:

$$v \leftarrow v + F^{(s)} \frac{\Delta t}{2m}$$

do $i = 1, n$

$$v \leftarrow v + F^{(f)} \frac{\delta t}{2m}$$

$$x \leftarrow x + v \delta t$$

$$v \leftarrow v + F^{(f)} \frac{\delta t}{2m}$$

end do

$$v \leftarrow v + F^{(s)} \frac{\Delta t}{2m}$$

Note that while the velocities will be updated on two different time scales, the positions will be updated using only the smallest time step. This is a direct consequence of choosing to segregate only the slow forces into $i\mathcal{L}_s$, and thus this type of rRESPA algorithm is referred to as a force-based split. This class of rRESPA propagators is applicable to a wide range of systems, and various forms of it have been used to accelerate simulations of water,¹⁹ ionic melts,²⁰ small organic molecules,^{6,7} buckminsterfullerene,⁸ proteins,^{3,9–11} Car–Parrinello dynamics,¹² and path integral molecular dynamics.⁵

B. Particle-based RESPA split

While a separation based on forces is perhaps the most widely used variant of the rRESPA algorithm, it is not the only one. Another common situation in MD simulations is to have some particles which are significantly lighter than the others. Since the particles' velocities will scale with the square root of their mass, it makes sense to devise a rRESPA propagator that takes advantage of this fact. In this case, the most convenient rRESPA propagator uses a division based on particles, instead of forces. The slow component of the Liouvillian will now contain the terms which affect either the positions or the velocities of the heavy particles,

$$i\mathcal{L}_s = \sum_{i \in \text{heavy}} \left[v_i \frac{\partial}{\partial x_i} + \frac{1}{2} \sum_{j \neq i} \frac{F_{ij}}{m_i} \frac{\partial}{\partial v_i} \right] \\ \equiv v_h \frac{\partial}{\partial x_h} + \frac{F_h}{m} \frac{\partial}{\partial v_h}, \quad (15)$$

and the fast component will contain the terms which affect the light particles,

$$i\mathcal{L}_f = \sum_{i \in \text{light}} \left[v_i \frac{\partial}{\partial x_i} + \frac{1}{2} \sum_{j \neq i} \frac{F_{ij}}{m_i} \frac{\partial}{\partial v_i} \right] \\ \equiv v_l \frac{\partial}{\partial x_l} + \frac{F_l}{m} \frac{\partial}{\partial v_l}. \quad (16)$$

After substituting these terms into the Trotter factorization of Eq. (7), the position and velocity terms in the exponents can be separated using a further Trotter expansion, which results in a propagator of the form

$$G(\Delta t) = \exp\left(\frac{\Delta t}{4} \frac{F_h}{m} \frac{\partial}{\partial v_h}\right) \exp\left(\frac{\Delta t}{2} v_h \frac{\partial}{\partial x_h}\right) \\ \times \exp\left(\frac{\Delta t}{4} \frac{F_h}{m} \frac{\partial}{\partial v_h}\right) \left[\exp\left(\frac{\delta t}{2} \frac{F_l}{m} \frac{\partial}{\partial v_l}\right) \exp\left(\delta t v_l \frac{\partial}{\partial x_l}\right) \right] \\ \times \exp\left(\frac{\delta t}{2} \frac{F_l}{m} \frac{\partial}{\partial v_l}\right) \right]^n \exp\left(\frac{\Delta t}{4} \frac{F_h}{m} \frac{\partial}{\partial v_h}\right) \\ \times \exp\left(\frac{\Delta t}{2} v_h \frac{\partial}{\partial x_h}\right) \exp\left(\frac{\Delta t}{4} \frac{F_h}{m} \frac{\partial}{\partial v_h}\right). \quad (17)$$

This is equivalent to the algorithmic prescription

$$v_h \leftarrow v_h + F_h \frac{\Delta t}{4m} \\ x_h \leftarrow x_h + v_h \frac{\Delta t}{2} \\ v_h \leftarrow v_h + F_h \frac{\Delta t}{4m} \\ \text{do } i = 1, n \\ v_l \leftarrow v_l + F_l \frac{\delta t}{2m} \\ x_l \leftarrow x_l + v_l \delta t \\ v_l \leftarrow v_l + F_l \frac{\delta t}{2m}$$

end do

$$v_h \leftarrow v_h + F_h \frac{\Delta t}{4m} \\ x_h \leftarrow x_h + v_h \frac{\Delta t}{2} \\ v_h \leftarrow v_h + F_h \frac{\Delta t}{4m}$$

Here, the positions are updated on both time scales, since the components of the Liouvillian were separated based on particle identity, and this class of rRESPA propagators is described as using a particle-based split. Propagators of this general form are also widely applicable, and have been used to simulate mixtures of light and heavy Lennard-Jones particles,² diatomic oscillators in a monatomic bath,^{2,13} polarizable ions in aqueous solution,^{14,15} and *ab initio* molecular dynamics.¹⁶

III. EXAMPLES

The two rRESPA propagators described in the previous section are presented merely as a framework for the discussion to follow—many other reversible propagators can also be constructed using the rRESPA technique.² For most applications, in fact, a choice must be made between several reasonable rRESPA propagators. Consider the case of a stiff oscillator in a slow-moving bath. One could either treat the oscillator as a light degree of freedom in a bath of heavy particles using Eq. (17),^{2,13} or separate the fast spring force from the slower forces acting in the bath using Eq. (13).⁵ In practice, there will be differences between these two approaches, in both the accuracy of the integration and the CPU time required by the simulation, and the correct choice depends on the nature of the system. By considering several examples in the sections to follow, we illustrate the importance of a properly chosen rRESPA split, and draw some conclusions about how to predict which rRESPA propagators will be most rewarding when treating novel systems.

A. Analytical treatment: Harmonic oscillator

Consider the model system depicted in Fig. 1. This system consists of a charge q , with mass m , moving in a harmonic potential with force constant $m\omega^2$. The particle also

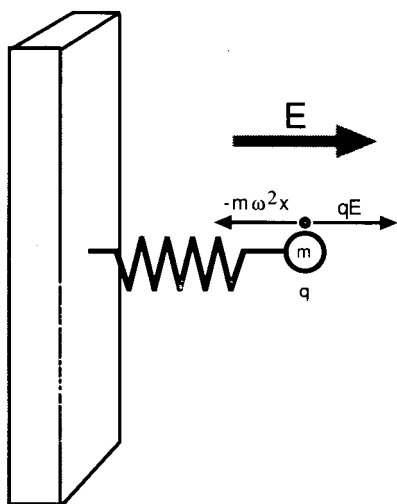


FIG. 1. One-dimensional model system with a fast linear force and a slow constant force.

feels a uniform electric field of strength E . This system will prove useful as a one-dimensional analog for a polarizable solute, but for now the important feature is that its dynamics can be solved analytically, facilitating a discussion of the errors induced by using approximate propagators of various types.

The single dynamical variable in this system is the position x of the charge. In terms of this variable, the potential is

$$V(x) = \frac{1}{2}m\omega^2x^2 - qEx, \quad (18)$$

and the trajectory is given by

$$x(t) = \frac{qE}{m\omega^2} + x_0 \cos(\omega t) + \frac{\dot{x}_0}{\omega} \sin(\omega t), \quad (19)$$

$$\dot{x}(t) = -x_0\omega \sin(\omega t) + \dot{x}_0 \cos(\omega t), \quad (20)$$

where $x_0 = x(0) - qE/m\omega^2$ is the particle's initial displacement from the minimum of the potential and $\dot{x}_0 = \dot{x}(0)$ is its initial velocity. These equations provide a standard against which we may compare the predictions of both the velocity Verlet and rRESPA propagators.

Using the rRESPA formalism, the velocity Verlet propagator²¹ can be generated by writing

$$G^{\text{vv}}(\Delta t) = e^{i\mathcal{L}_v\Delta t/2} e^{i\mathcal{L}_x\Delta t} e^{i\mathcal{L}_v\Delta t/2}, \quad (21)$$

where

$$i\mathcal{L}_v = \frac{F}{m} \frac{\partial}{\partial \dot{x}} = - \left(x - \frac{qE}{m\omega^2} \right) \omega^2 \frac{\partial}{\partial \dot{x}} \quad (22)$$

represents the part of the Liouvillian that acts on the particle's velocity, and

$$i\mathcal{L}_x = \dot{x} \frac{\partial}{\partial x} \quad (23)$$

represents the part of the Liouvillian that acts on its position. The propagator G^{vv} is identical to the usual velocity Verlet integrator, which for our shifted harmonic oscillator can be written as

$$x(\Delta t) = \frac{qE}{m\omega^2} + x_0 + \dot{x}_0\Delta t - \frac{1}{2}x_0\omega^2\Delta t^2, \quad (24)$$

$$\dot{x}(\Delta t) = \dot{x}_0 - x_0\omega^2\Delta t - \frac{1}{2}\dot{x}_0\omega^2\Delta t^2 + \frac{1}{4}x_0\omega^4\Delta t^3. \quad (25)$$

Note that these equations match the Taylor expansions of Eqs. (19) and (20) exactly through terms of $\mathcal{O}(\Delta t^2)$, confirming that the error in a velocity Verlet trajectory is of $\mathcal{O}(\Delta t^3)$. More specifically, the leading terms in the trajectory errors after one time step are

$$\Delta x^{\text{vv}} = \frac{1}{6}\dot{x}_0\omega^2\Delta t^3, \quad (26)$$

$$\Delta \dot{x}^{\text{vv}} = \frac{1}{12}x_0\omega^4\Delta t^3. \quad (27)$$

Note that for any trajectory which oscillates symmetrically through the minimum of the potential, these errors will average to zero over time, guaranteeing a stable simulation.

If we wish to use rRESPA on this system, it would seem natural to separate the "fast" spring force from the "slow" constant force due to the electric field, using a force-based propagator as given by Eq. (13). This turns out to be a mistake in certain circumstances, for reasons which will become clear in a moment. To illustrate this point, we proceed to partition the Liouvillian such that

$$i\mathcal{L}_s = \frac{qE}{m} \frac{\partial}{\partial \dot{x}}; \quad (28)$$

$$i\mathcal{L}_f = \dot{x} \frac{\partial}{\partial x} - \omega^2x \frac{\partial}{\partial \dot{x}}. \quad (29)$$

To permit us to concentrate only on the errors associated with the rRESPA split, we make use of a propagator of the form

$$G(\Delta t) = e^{i\mathcal{L}_s\Delta t/2} e^{i\mathcal{L}_f\Delta t} e^{i\mathcal{L}_s\Delta t/2} \quad (30)$$

with no further factorization of the inner term. Using an analytical solution for the dynamics generated by the inner propagator is equivalent to taking $\delta t \rightarrow 0$, and eliminates all of the errors except those associated with the separation of time scales.²² This results in an integrator of the form

$$x(\Delta t) = \left(x_0 + \frac{qE}{m\omega^2} \right) \cos(\omega\Delta t) + \left(\frac{\dot{x}_0}{\omega} + \frac{1}{2} \frac{qE}{m\omega^2} \omega\Delta t \right) \sin(\omega\Delta t), \quad (31)$$

$$\dot{x}(\Delta t) = - \left(x_0 + \frac{qE}{m\omega^2} \right) \omega \sin(\omega\Delta t) + \frac{1}{2} \frac{qE}{m\omega^2} \omega^2\Delta t - \left(\dot{x}_0 + \frac{1}{2} \frac{qE}{m\omega^2} \omega^2\Delta t \right) \cos(\omega\Delta t). \quad (32)$$

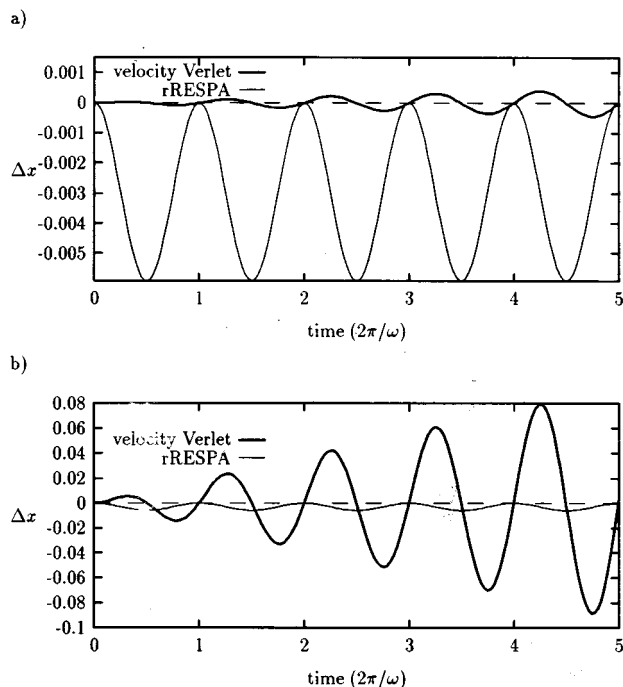


FIG. 2. Errors in the trajectory of a charged harmonic oscillator in a constant electric field when propagated by velocity Verlet (bold lines) and rRESPA (thin lines). Time step for each method is $0.03 \times 2\pi/\omega$. The quantity plotted is the deviation from the analytically correct trajectory. (a) Maximum kinetic energy $= q^2 E^2 / 20000 m \omega^2$. (b) Maximum kinetic energy $= 2 q^2 E^2 / m \omega^2$. Note the difference in scale. The increasing errors in the velocity Verlet simulations represent a dephasing of the trajectory, not an instability.

When the Taylor expansions of these equations are compared to the Taylor expansions of the exact propagator [Eqs. (19) and (20)], the leading terms in the RESPA errors are seen to be

$$\Delta x^R = -\frac{1}{24} \frac{qE}{m\omega^2} \omega^4 \Delta t^4, \quad (33)$$

$$\Delta \dot{x}^R = -\frac{1}{12} \frac{qE}{m\omega^2} \omega^4 \Delta t^3. \quad (34)$$

Comparing these errors to those generated by the velocity Verlet algorithm [Eqs. (26) and (27)], we see two important differences. The leading term in the rRESPA position error is only $\mathcal{O}(\Delta t^4)$, suggesting that rRESPA has the potential to generate a more accurate trajectory. Equally important, however, is the fact that the rRESPA errors are systematically negative. Unlike the velocity Verlet errors, which average to zero over a full period of the oscillator, the predicted rRESPA positions and velocities will be consistently more negative than the analytically correct values.²³ Which of these two factors will dominate the dynamics depends upon how strong the slow force is relative to the fast force.

These differences between velocity Verlet and rRESPA are illustrated in Fig. 2, which shows the error in the trajectory for these two propagators. When the kinetic energy is low, the particle spends all of its time stretched away from the origin by the electric field. Thus the fast spring force

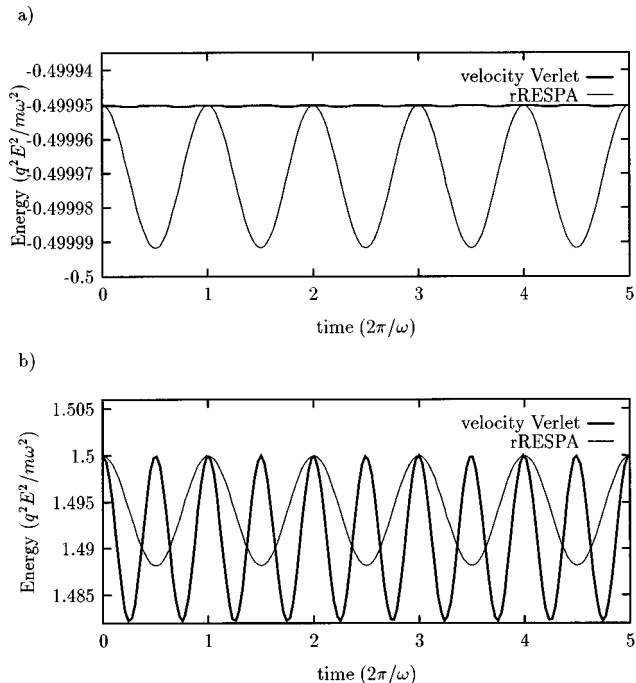


FIG. 3. Energy trace for the trajectory of a charged harmonic oscillator in a constant electric field when propagated by velocity Verlet (bold lines) and rRESPA (thin lines). Time step for each method is $0.03 \times 2\pi/\omega$. (a) Maximum kinetic energy $= q^2 E^2 / 20000 m \omega^2$. (b) Maximum kinetic energy $= 2 q^2 E^2 / m \omega^2$. Note the difference in scale.

consistently opposes, and is nearly equal to, the slow force from the electric field. Even though the slow force is constant, treating it on a different time scale than the spring force can induce considerable errors, as shown in Fig. 2(a). When the kinetic energy is large, however, the spring will oscillate through the minimum of the potential, and the spring force will not act in a consistent direction relative to the force due to the electric field. In this case, the errors in the rRESPA propagator can be smaller than those from velocity Verlet, and the trajectory more stable, as in Fig. 2(b). The energy traces for these two cases are displayed in Fig. 3, showing that rRESPA can also provide energy conservation that is either better or worse than velocity Verlet, again depending on the importance of the slow force. Note, however, that both propagators generate stable trajectories with no drift in the energy.

The conclusion we may draw at this point is a rather obvious one, which will be echoed in the more realistic examples to follow: A subdivision of the Liouvillian will fail if the slow and the fast forces are of similar magnitude and consistently opposing each other. This is a rather basic principle, which has been pointed out before, and is implicit in the terminology of a ‘reference’ and a ‘correction’ propagator.² These equal and opposite forces become more difficult to spot in more complicated systems, however, and the application of this principle is not always so obvious.

B. Polarizable ions

Although the model in the previous section was chosen primarily for its simplicity, it is also a useful analog for

several physical systems. The fast oscillator in a slowly varying field can represent a diatomic molecule in a slow bath,^{2,13} or the dipolar degrees of freedom in an extended-Lagrangian polarizable MD simulation.^{14,15,24,25} These two cases, in fact, correspond quite well to the two sets of conditions in the previous section. In the case of a diatomic solute, the oscillator is typically in thermal equilibrium with the rest of the bath. The intramolecular bond will thus vibrate through the zero of the potential as in Figs. 2(b) and 3(b), and the separation of forces should cause no problem. When the oscillator is a polarizable point dipole, however, its kinetic energy is usually kept quite low, in order to keep the dipole near its optimum value.^{14,15,24} Consequently, the force from the bath will consistently oppose the spring force as in Figs. 2(a) and 3(a), and the rRESPA split describe in the previous section would be expected to fail.

To illustrate this, we consider a system consisting of a polarizable chloride ion solvated by a cluster of 255 water molecules. (A finite system is chosen in order to eliminate any energy conservation issues associated with cutoffs or Ewald sums.) The simulation details have been described previously;^{14,15} we summarize them only briefly here. The water model used is the four-point transferable intermolecular potential (TIP4P) of Jorgensen *et al.*²⁶ The model for Cl⁻ is a Drude oscillator^{27,28} with a net charge of $-1|e|$ which interacts with the water molecules via Coulomb and Lennard-Jones interactions. These Drude ions are maintained at extremely low temperatures (<1 K) by periodically quenching their velocities, so that they provide an accurate representation of the instantaneous ionic dipole moments. This model is similar in many ways to the ionic shell model,²⁹ which has also been used to model systems of polarizable ions.

The rRESPA split which corresponds to the model system of the previous section involves placing the slowly varying forces in the slow part of the propagator, and the quickly varying spring forces in the fast part. Thus we define

$$F_{ij}^{(f)} = \delta_i^D \delta_j^D F_{ij}; \quad (35)$$

$$F_{ij}^{(s)} = F_{ij} - F_{ij}^{(f)}, \quad (36)$$

where δ_i^D is a delta function which discriminates between Drude ions and atoms in other types of molecules,

$$\delta_i^D = \begin{cases} 1, & i \in \text{Drude ion} \\ 0, & \text{otherwise.} \end{cases} \quad (37)$$

This force-based split is used in the rRESPA propagator of Eq. (13), with an outer time step of $\Delta t = 1$ fs and an inner time step of $\delta t = \Delta t/4 = 0.25$ fs, with the results shown in Fig. 4(a). Also shown is an energy trace from a velocity Verlet simulation with $\Delta t = 1$ fs, which results in considerably better energy conservation.

As predicted, separating the spring force and the bath force is counterproductive in this case. Since the spring is kept cold, the bath force is constantly acting to stretch the Drude spring, maintaining a persisting opposition between spring and bath forces, which results in an accumulation of errors. A better alternative would be to put the forces from

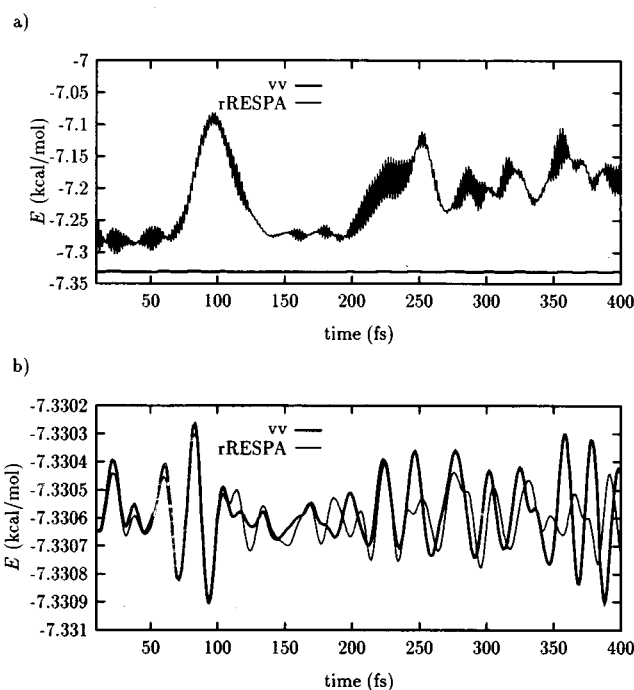


FIG. 4. Energy trace for a simulation of Drude chloride ion in TIP4P water for both velocity Verlet (bold lines) and rRESPA (thin lines) propagators. (a) Ion-water interactions in outer rRESPA propagator. (b) Ion-water interactions in inner rRESPA propagator. Note the difference in scale.

the ion-water interactions in the inner propagator, together with the spring forces that they oppose. This requires a larger number of interactions to be evaluated in the inner propagator, but ensures that the slow force will not always act in the same direction relative to the Drude spring vector. With the force separation modified to have the form

$$F_{ij}^{(s)} = (1 - \delta_i^D)(1 - \delta_j^D)F_{ij}; \quad (38)$$

$$F_{ij}^{(f)} = F_{ij} - F_{ij}^{(s)}. \quad (39)$$

and with $\Delta t = 1$ fs and $\delta t = 0.25$ fs as before, the simulation results are as shown in Fig. 4(b). This time the rRESPA algorithm provides energy conservation directly comparable to that of velocity Verlet, with CPU times that are nearly four times faster.

C. Ewald

Another situation for which this sort of analysis proves useful is in systems which use Ewald summation. Since Ewald sums are used to evaluate long-ranged Coulombic interactions, it seems natural to use them as a basis for separating near (fast) and far (slow) forces in a rRESPA split. A straightforward application of this idea does indeed provide a noticeable speedup,¹¹ but a careful examination shows that a slightly less obvious split provides for an even more efficient propagator.

In general, the technique of Ewald sums³⁰ is useful in systems with large partial charges, since the long-ranged Coulomb interactions do not converge sufficiently when

summed over a single unit cell. The slowly (and conditionally) converging sum of electrostatic interactions

$$V^{\text{el}} = \frac{1}{2} \sum_{\mathbf{n}} \sum_i \sum_j' \frac{q_i q_j}{|\mathbf{r}_{ij} + \mathbf{n}|} \quad (40)$$

is rearranged so that part of it is summed in real space, and the rest is summed in Fourier space,³¹

$$\begin{aligned} V^{\text{el}} = & \frac{1}{2} \sum_i \sum_{j \neq i} q_i q_j \frac{\text{erfc}(\kappa r_{ij})}{r_{ij}} \\ & + \frac{1}{2} \sum_i \sum_j \sum_{\mathbf{k} \neq 0} \frac{1}{\pi L^3} \frac{4\pi^2}{k^2} q_i q_j e^{-k^2/4\kappa^2} \cos \mathbf{k} \cdot \mathbf{r}_{ij} \\ & - \frac{\kappa}{\sqrt{\pi}} \sum_i q_i^2. \end{aligned} \quad (41)$$

With a suitable choice for the screening parameter κ , both sums can be made to converge reasonably quickly.³² More specifically, κ is always chosen so that the first term in the expression above (the real-space sum) is adequately converged within a radius of no more than $r = L/2$, where L is the side length of the cubic unit cell. Therefore, the first term includes primarily short-ranged interactions. The second term (the k -space sum), on the other hand, results from a Fourier expansion of the potential due to an infinite array of Gaussian charges, much of which is considerably longer-ranged than the real-space sum. Under the usual assumption that long-ranged forces may be updated less frequently than short-ranged forces, it thus seems reasonable to separate the real- and k -space sums in a rRESPA split. For example, if we rewrite the Ewald sum in the form

$$V^{\text{el}} = \frac{1}{2} \sum_i \sum_j V_{ij}^{\text{el}}, \quad (42)$$

where

$$\begin{aligned} V_{ij}^{\text{el}} = & q_i q_j \left[(1 - \delta_{ij}) \frac{\text{erfc}(\kappa r_{ij})}{r_{ij}} \right. \\ & \left. + \frac{1}{\pi L^3} \sum_{\mathbf{k} \neq 0} \frac{4\pi^2}{k^2} e^{-k^2/4\kappa^2} \cos \mathbf{k} \cdot \mathbf{r}_{ij} - \delta_{ij} \frac{2\kappa}{\sqrt{\pi}} \right], \end{aligned} \quad (43)$$

then we can separate the real-space and k -space parts of the potential,

$$V_{ij}^{\text{el}} = V_{ij}^{\text{rs}} + V_{ij}^{\text{ks}}, \quad (44)$$

with

$$V_{ij}^{\text{rs}} = (1 - \delta_{ij}) q_i q_j \frac{\text{erfc}(\kappa r_{ij})}{r_{ij}} \quad (45)$$

and

$$V_{ij}^{\text{ks}} = q_i q_j \left[\frac{1}{\pi L^3} \sum_{\mathbf{k} \neq 0} \frac{4\pi^2}{k^2} e^{-k^2/4\kappa^2} \cos \mathbf{k} \cdot \mathbf{r}_{ij} - \delta_{ij} \frac{2\kappa}{\sqrt{\pi}} \right]. \quad (46)$$

With these definitions, we may define a rRESPA split with

$$\mathbf{F}_{ij}^{(f)} = -\nabla_{\mathbf{r}_{ij}} V_{ij}^{\text{rs}} \quad (47)$$

and

$$\mathbf{F}_{ij}^{(s)} = -\nabla_{\mathbf{r}_{ij}} V_{ij}^{\text{ks}}, \quad (48)$$

and use Eq. (13) to propagate the dynamics. (The real-space forces could also be further subdivided into distance classes, if desired.) Such an approach seems perfectly reasonable, given the disparity in distances over which the terms in the real- and k -space sums act. Indeed, an approach very similar to this has been used recently in large-scale Ewald simulations of proteins.¹¹

Although this particular rRESPA split is moderately successful, it is not necessarily the best choice. The reason for this is that the “long-ranged” k -space sum still contains some fraction of *every* pair interaction, even the most short-ranged. For typical values of the screening parameter κ , even nearest-neighbor Coulomb interactions can be diminished significantly (20%–40%) by the complementary error function in the real-space sum. This screened amount is then evaluated in the k -space sum, which is the “slow” piece of the propagator described above. The presence of these short-ranged interactions in the k space sum will limit the size of the large time step Δt more than would be necessary if the slow piece of the propagator were truly long ranged. Indeed, in the published report which uses this propagator, the k -space forces required a time step which was shorter than that used for some of the real-space forces.¹¹

As in the previous two examples, this rRESPA propagator can be seen to produce a persistent opposition between two important forces in the system. This is illustrated graphically in Fig. 5. For configurations where a molecule is roughly stationary with respect to one (or more) of its neighbors, the repulsive Lennard-Jones (LJ) forces will approximately cancel the attractive electrostatic forces. When the forces are divided into separate slow (k -space) and fast (real-space and LJ) contributions, there will be a similar cancellation between the fast and slow forces. More significantly, the fast forces will be consistently repulsive and the slow forces consistently attractive. This situation will persist for as long as the two molecules in question remain closely bound. In systems with strong hydrogen bonds (which can persist for thousands of time steps) the stage is then set for the same type of systematic errors that were observed in the previous two sections.

A better alternative would be to assign the *entire* Coulomb interaction between nearby atom pairs to the fast propagator, including both real- and k -space contributions. Forces acting between distant atoms can then be assigned to the slow propagator. Thus all pair forces are subdivided based on the basis of the distance over which they act, regardless of whether they are real-space or k -space forces. Somewhat surprisingly, this can be implemented with less computation than for the real-space/ k -space split described above. This is done by first dividing the electrostatic pair energy of Eq. (43) into a contribution from the central unit

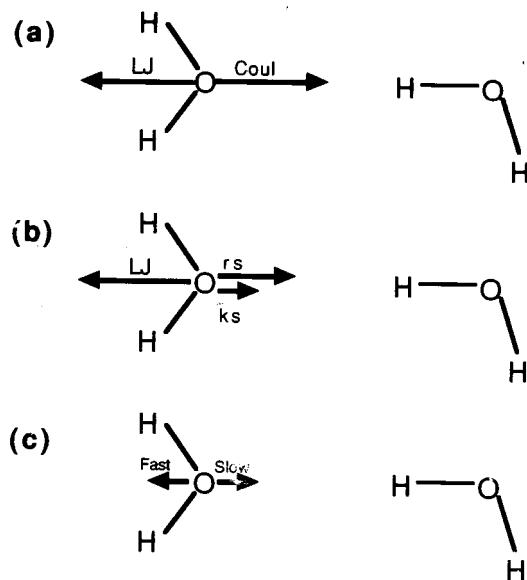


FIG. 5. Illustration of the opposing forces generated by a real-space/ k -space split of the Ewald interactions. (a) Lennard-Jones and Coulomb forces will largely cancel for a pair of hydrogen-bonded molecules. (b) Roughly 2/3 of the Coulomb interaction will be included in the real-space term, the rest will be included in the k -space sum. (c) If the k -space terms are all included in the slow propagator, there will be a persistent opposition between the two halves of the rRESPA propagator with respect to the molecular axis.

cell ($\mathbf{n}=\mathbf{0}$) and another from all image cells ($\mathbf{n}\neq\mathbf{0}$). The $\mathbf{n}=\mathbf{0}$ contribution is equivalent to the usual minimum-image boundary conditions,

$$V_{ij}^0 = (1 - \delta_{ij}) \frac{q_i q_j}{r_{ij}}, \quad (49)$$

and the contribution from higher \mathbf{n} contains the remaining terms in Eq. (43),

$$V_{ij}^n = q_i q_j \left[-(1 - \delta_{ij}) \frac{\text{erf}(\kappa r_{ij})}{r_{ij}} + \sum_{\mathbf{k}\neq\mathbf{0}} \frac{1}{\pi L^3} \frac{4\pi^2}{k^2} e^{-k^2/4\kappa^2} \cos \mathbf{k}\cdot\mathbf{r}_{ij} - \delta_{ij} \frac{2\kappa}{\sqrt{\pi}} \right], \quad (50)$$

so that

$$V_{ij}^{\text{el}} = V_{ij}^0 + V_{ij}^n \quad (51)$$

Note that the calculation of V^n is nearly equivalent to the calculation of the full Ewald sum, with the substitution of a standard error function for its complement. Thus V^n is significantly more expensive to compute than V^0 , which involves no special functions and can even be obtained at no cost during the time steps in which V^n must be calculated. Furthermore, all of the terms in V_{ij}^n are truly long ranged, acting at distances of at least $L/2$. This is the ideal situation for a rRESPA split, since the most expensive part of the calculation is also the most long-ranged.

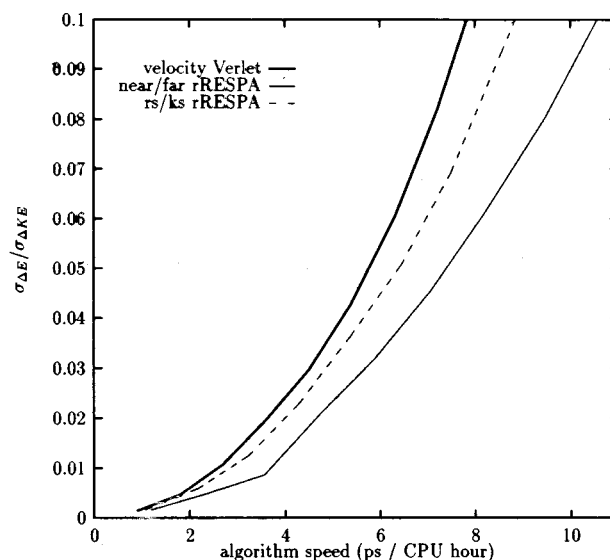


FIG. 6. Energy conservation as a function of algorithm speed for velocity Verlet (bold line), near/far rRESPA (thin line), and real space/ k -space rRESPA (dashed line).

Using this division of the potential, we can define a rRESPA split which separates the fast force due to only the most short-ranged interactions,

$$\mathbf{F}_{ij}^{(f)} = -S(r_{ij}) \nabla_{\mathbf{r}_{ij}} V_{ij}^0, \quad (52)$$

from the remaining slow forces,

$$\mathbf{F}_{ij}^{(s)} = -[1 - S(r_{ij})] \nabla_{\mathbf{r}_{ij}} V_{ij}^0 - \nabla_{\mathbf{r}_{ij}} V_{ij}^n, \quad (53)$$

where the switching function $S(r)$ is equal to unity at $r=0$, and smoothly decreases to zero beyond some cut-off distance. The use of a switching function is a common method used to minimize the energy conservation errors that are typically associated with abrupt cutoffs, such as the one implicit in V_{ij}^0 .³³ This subdivision of the forces can then be used in the force-split rRESPA propagator of Eq. (13).

To demonstrate that this near/far rRESPA split is indeed more efficient than the real space/ k -space split, we have applied both propagators, as well as velocity Verlet, to simulate a system of 256 TIP4P water molecules at 298 K and a density of 1.0 g/mL ($L=19.71$ Å). Ewald sums were used with $\kappa=6.0/L$ and 257 k vectors. The switching function $S(r)$ was chosen to be a cubic spline with first derivatives equal to zero at $r=6$ Å and $r=10$ Å. All LJ and real-space Coulomb interactions were terminated beyond $r=9.85$ Å $\approx L/2$ in both the rRESPA and the velocity Verlet simulations.

Each of the three propagators (velocity Verlet, near/far rRESPA and real-space/ k -space rRESPA) was used in a series of 8 ps simulations with varying time steps. For the rRESPA simulations, n was chosen to be 2 in Eq. (13), so that $\delta t = \Delta t/2$. The energy conservation of each of these runs is plotted in Fig. 6 against the number of picoseconds which can be simulated in one CPU hour on an IBM RS/6000 590. This makes it easy to compare the speed of the different

algorithms at a constant level of energy conservation. Energy conservation is defined here as the root mean square single-step energy error, normalized by the root mean square single-step change in the kinetic energy,

$$\frac{\sigma_{\Delta E}}{\sigma_{\Delta KE}} = \frac{\langle (E(t+\Delta t) - E(t))^2 \rangle^{1/2}}{\langle (KE(t+\Delta t) - KE(t))^2 \rangle^{1/2}}, \quad (54)$$

where the averages are performed over the length of the simulation.³⁴ A value of 0.02, for example, means that the fluctuations in the total system energy are 2% as large as the fluctuations in the kinetic energy.

The important quantity to notice in Fig. 6 is the ratio of each rRESPA speed to the speed of the velocity Verlet algorithm at a given level of energy conservation; this represents the speedup attributable to the method in question. Calculating this ratio shows that the near/far rRESPA split is 25% to 35% faster than velocity Verlet, whereas the real space/*k*-space split produces only an 11% speedup. While neither of these numbers is very impressive (both would improve for larger systems and a multilevel rRESPA split) this demonstrates that a carefully constructed rRESPA propagator can provide two to three times the benefit of a more obvious choice.

D. Hot/cold system

As a final example, we consider the ‘‘hot/cold’’ system described in a recent paper.¹⁷ This system consists of small number of extremely hot (i.e., fast-moving) particles surrounded by a bath of cooler particles, and is relevant in the study of relaxation dynamics following photoexcitation. Using traditional propagators, a very small time step must be used to integrate this system, due to the presence of the fast-moving particles. With a properly chosen rRESPA split, however, much of the system’s dynamics can be integrated with a larger time step offering considerable savings in CPU time.¹⁷

As usual, there are several different rRESPA propagators which can be applied to this system. And once again, they may be evaluated by considering the effect they have on the forces in the system.

Since the objective is to integrate the dynamics of the hot particles with a smaller time step than the cold particles, the most obvious choice for a rRESPA propagator is to use a particle-based split as described in Sec. II B, with each particle assigned to a piece of the propagator based on its velocity,

$$i\mathcal{L}_f = \sum_i \left[v_i \frac{\partial}{\partial x_i} + \frac{F_i}{m_i} \frac{\partial}{\partial v_i} \right] \theta(|v_i| - v^*); \quad (55)$$

$$i\mathcal{L}_s = \sum_i \left[v_i \frac{\partial}{\partial x_i} + \frac{F_i}{m_i} \frac{\partial}{\partial v_i} \right] \theta(v^* - |v_i|), \quad (56)$$

where v^* is a threshold velocity which is used to define the ‘‘hot’’ atoms, and $\theta(x)$ is the unit step function,

$$\theta(x) = \begin{cases} 0, & x < 0 \\ 1, & x > 0 \end{cases} \quad (57)$$

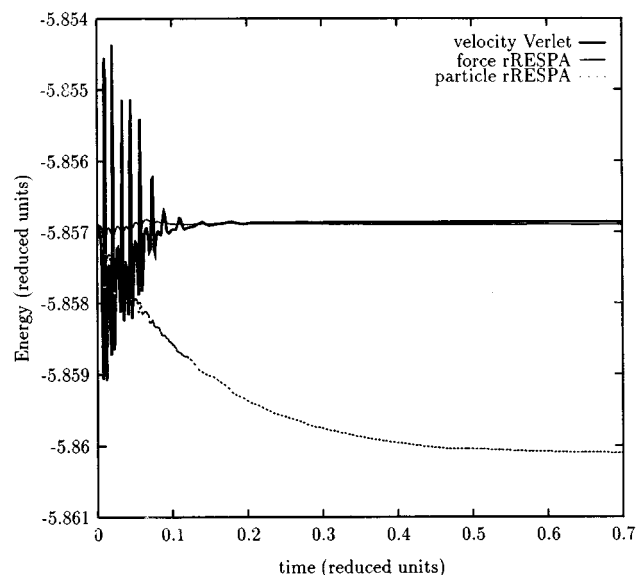


FIG. 7. Energy trace for a simulation of 4000 Lennard-Jones particles, one of which initially has a kinetic energy 10 000 times larger than the average KE of the remaining particles. Curves shown are for velocity Verlet with $\Delta t=0.001$ reduced time units (bold line), a rRESPA particle split [see Eqs. (55) and (56)] with $\Delta t=0.004$ and $\delta t=0.001$ (dotted line) and a rRESPA force split [see Eqs. (58) and (59)] with $\Delta t=0.004$ and $\delta t=0.001$ (thin line).

This rRESPA split turns out to be less than ideal, however, when we consider its effects more carefully. The strongest forces in the system will be experienced during the collisions involving hot atoms, since these are the most energetic particles. In particular, the collisions between hot and cold atoms will typically be quite forceful. In these collisions, however, the subdivision of the Liouvillian proposed in Eqs. (55) and (56) will place one part of the collision force in the fast propagator and its reaction force in the slow propagator. As we have seen from the examples in the preceding sections, separating strong and opposing forces in this way typically leads to poor energy conservation. This principle holds true for the current case as well, as shown in Fig. 7: The energy conservation for a 4000-particle Lennard-Jones system with one initially hyperkinetic particle is considerably worse with a rRESPA particle-based split than it is for velocity Verlet over the duration of the reequilibration period, and has a noticeable drift.

To avoid this problem, we must find a rRESPA split which puts all reciprocal force pairs involving the hot atoms into the same piece of the propagator. This can be accomplished with a force-based split of the form

$$F_{ij}^{(s)} = \theta(v^* - |v_i|) \theta(v^* - |v_j|) F_{ij}; \quad (58)$$

$$F_{ij}^{(f)} = [1 - \theta(v^* - |v_i|) \theta(v^* - |v_j|)] F_{ij}. \quad (59)$$

Note that all forces between pairs of hot atoms, as well as those between hot and cold atoms, have been assigned to the fast piece of the Liouvillian; the cold–cold forces (a majority of the interactions) are assigned to the slow piece of the Liouvillian. A propagator can then be constructed as in Eq.

(13). The energy conservation with this propagator is significantly improved from both velocity Verlet and the previous rRESPA propagator, as shown in Fig. 7.

We should note, however, that there are other problems associated with this particular type of rRESPA propagator. These arise as a result of the step functions in Eqs. (58) and (59). The purpose of these step functions is to discriminate between two classes of forces in order to determine when they should be applied in the rRESPA propagator. Since the velocities upon which this decision is based can change at two points during each small time step, as well as two during each large time step, these forces should be repartitioned as often as $2n+2$ times per large time step. [Cf. Eq. (13) and the algorithm which follows it.] This introduces considerable algorithmic complexity which we prefer to avoid. Instead, the approach taken in Ref. 17 was to classify the atoms as hot or cold only once per large time step. While this simplifies and speeds up the MD simulation, it has the side effect of making the discriminant step functions in Eqs. (58) and (59) nonlocal in time, thereby destroying the reversibility of the algorithm. This has the unwelcome result of inducing a slight drift at times longer than those shown in Fig. 7. For systems in which this would be a problem, the solution would be to use a fully local implementation of Eqs. (58) and (59); this would require a careful implementation to avoid storage or recalculation of the $N \times N$ force array, and would be somewhat slower than the current implementation. Furthermore, a fully local implementation appears to require the use of a smooth switching function in place of the abrupt cutoffs in Eq. (58) and (59); this is analogous to the case for distance cutoffs, such as those in Eqs. (52) and (53).

IV. CONCLUSION

Each of the four examples considered above provides a different illustration of a rRESPA propagator that does not work as well as expected. In each case, the flaw was attributed to an important force in the system which was separated from an opposing force of some kind, and integrated with different time step. While this is an important observation, it alone is not enough to determine *a priori* which rRESPA splits will be efficient. Indeed, it is something of a tautology: Every conservative system has a net force of zero, so that any RESPA split will necessarily separate equal and opposing forces. For these observations to have more predictive value, we must consider particle- and force-based splits separately.

The hot/cold system discussed in Sec. III D provides one example of a particle-based rRESPA split. For this system, a particle-based split was less advantageous than a force-based split since it separated equal and opposite forces acting between colliding atoms. Since any particle-based split will separate some paired reaction forces in this manner, one may well wonder why it is that all particle-based rRESPA splits do not fail.

Examples in the literature which do successfully implement a particle-based rRESPA split^{2,14-16} have one feature in common: They all make use of a fast subsystem which con-

tains extremely light particles. These particles are typically 10 to 100 times lighter than the heavy particles in the system, and often represent electronic degrees of freedom.¹⁴⁻¹⁶ Although there is still a separation of equal and opposing forces between the two subsystems during every light/heavy collision, these collisions have a relatively minor impact on the trajectories of the heavy particles, since the light particles have smaller momenta. The effect on the light particles is large, of course, but these particles are being integrated with the smaller time step. We suggest restricting the use of a particle-based rRESPA split to cases where the disparity in masses between light and heavy particles is at least a factor of 10.

For force-based splits, the issue is a little different. Due to the nature of this rRESPA split, each pair of equal and opposing forces will remain in the same piece of the propagator—no force will be integrated separately from its direct reaction force. The problem arises here when one broadly defined type of force is separated from a different type which consistently opposes it. In some cases the opposition between these forces is immediately apparent, as in the harmonic restoring force of Secs. III A and III B. Sometimes a persistent opposition between two forces can be more subtle, however, as with the Lennard-Jones and k -space Ewald forces in Sec. III C. In these situations there is no substitute for a certain amount of physical intuition about the system being studied. One must consider the various forces in the system and where they are being placed in the rRESPA split. If there is a physical reason why one type of force should oppose a force which is being integrated with a different time step, one should be extremely cautious. If this opposition is temporary, and will be erased over the time scale of a molecular collision, for example, then there is less cause for concern. But if the opposition persists over longer time scales, then the energy conservation and trajectory will likely suffer as a result, and a different rRESPA split should be considered.

Some of the most successful uses of the rRESPA method have combined several different rRESPA splits in a nested algorithm.^{3,6,8-11} For these cases, the guidelines developed above should be applied to each subdivision of the Liouvillian. If the forces are separated based on several different criteria (e.g., distance and force type^{3,6,8-11}), then care should be taken that any consistently opposing forces are integrated with the same time step. And a combined mass and force split requires a system with both a tenfold (or greater) mass difference between light and heavy particles as well as separable, nonopposing forces.

The factorization of the classical propagator used in rRESPA is a very powerful method, which can accelerate simulations by factors of 4 to 15. It can, however, introduce errors which are not present in standard MD algorithms, and some care is required to ensure that these do not pose a problem. By illustrating some of the pitfalls that can result from incautious application of the rRESPA method, we hope to make them easier for others to avoid when using rRESPA on previously untreated systems.

ACKNOWLEDGMENTS

This work supported by the NSF (CHE-91-22506) and the Maui High Performance Computing Center.

- ¹L. Greengard and V. Rokhlin, *J. Comput. Phys.* **60**, 187 (1985).
- ²M. Tuckerman, B. J. Berne, and G. J. Martyna, *J. Chem. Phys.* **97**, 1990 (1992).
- ³R. Zhou and B. J. Berne, *J. Chem. Phys.* **103**, 9444 (1995).
- ⁴Using the Moore's Law assumption that computer chip speed doubles every 18 months.
- ⁵M. E. Tuckerman, B. J. Berne, G. J. Martyna, and M. L. Klein, *J. Chem. Phys.* **99**, 2796 (1993).
- ⁶M. Watanabe and M. Karplus, *J. Chem. Phys.* **99**, 8063 (1993).
- ⁷M. E. Tuckerman and W. Langel, *J. Chem. Phys.* **100**, 6368 (1994).
- ⁸P. Procacci and B. J. Berne, *J. Chem. Phys.* **101**, 2421 (1994).
- ⁹D. D. Humphreys, R. A. Friesner, and B. J. Berne, *J. Phys. Chem.* **98**, 6885 (1994).
- ¹⁰M. Karplus and M. Watanabe, *J. Phys. Chem.* **99**, 5680 (1995).
- ¹¹P. Procacci and M. Marchi, *J. Chem. Phys.* **104**, 3003 (1996).
- ¹²M. E. Tuckerman and M. Parrinello, *J. Chem. Phys.* **101**, 1302 (1994).
- ¹³M. Tuckerman and B. J. Berne, *J. Chem. Phys.* **98**, 7301 (1993).
- ¹⁴S. J. Stuart, Ph.D. thesis, Columbia University, New York, NY, (1995).
- ¹⁵S. J. Stuart and B. J. Berne, *J. Chem. Phys.* (submitted).
- ¹⁶D. A. Gibson and E. A. Carter, *J. Phys. Chem.* **97**, 13429 (1993).
- ¹⁷R. Zhou, S. J. Stuart, and B. J. Berne, *J. Chem. Phys.* (in press, 1996).
- ¹⁸H. F. Trotter, *Proc. Am. Math. Soc.* **10**, 545 (1959).
- ¹⁹M. Tuckerman and B. J. Berne (unpublished results).
- ²⁰S. Rick and B. J. Berne (unpublished results).
- ²¹W. C. Swope, H. C. Andersen, P. H. Berens, and K. R. Wilson, *J. Chem. Phys.* **76**, 637 (1982).
- ²²This algorithm is thus more properly termed reversible NAPA, instead of reversible RESPA (see Ref. 2).
- ²³The errors will still be self-correcting, however, and the trajectory will be stable: $\Gamma(t + \Delta t)$ will always deviate in a negative direction from the *perturbed* trajectory, but may still coincide with the analytically correct trajectory. See Fig. 2.
- ²⁴M. Wilson and P. A. Madden, *J. Phys.: Condens. Matter* **5**, 2687 (1993).
- ²⁵P. J. Mitchell and D. Fincham, *J. Phys.: Condens. Matter* **5**, 1031 (1993).
- ²⁶W. L. Jorgensen, J. Chandrasekhar, J. D. Madura, R. W. Impey, and M. L. Klein, *J. Chem. Phys.* **79**, 926 (1983).
- ²⁷J. Hoye and G. Stell, *J. Chem. Phys.* **73**, 461 (1980).
- ²⁸L. R. Pratt, *Mol. Phys.* **40**, 347 (1980).
- ²⁹M. J. L. Sangster and M. Dixon, *Adv. Phys.* **23**, 247 (1976).
- ³⁰P. Ewald, *Ann. Phys.* **64**, 253 (1921).
- ³¹D. M. Heyes, *J. Chem. Phys.* **74**, 1924 (1981).
- ³²D. Fincham, *Inform. Q. Comput. Simulation Condensed Phases* **38**, 17 (1993).
- ³³M. E. Tuckerman, B. J. Berne, and G. J. Martyna, *J. Chem. Phys.* **94**, 6811 (1991).
- ³⁴Although related, this quantity is not the same as the more familiar root mean square deviation in the total energy (σ_E/σ_{KE}) (Ref. 36). We have found that the distribution of single-step energy errors is a more reliable method for distinguishing between energy errors due to enhanced fluctuations and those due to drifts. We hope to comment in more detail on these issues in a future publication.
- ³⁵L. Perera and M. Berkowitz, *J. Chem. Phys.* **100**, 3085 (1994).
- ³⁶W. F. van Gunsteren and H. J. C. Berendsen, *Mol. Phys.* **34**, 1311 (1977).